International Journal on Advanced Science Engineering Information Technology

Vol.8 (2018) No. 6
ISSN: 2088-5334

Antibacterial Inactivation of Escherichia coli after TiO2-Fe3O4-Bentonite Photocatalytic Treatment

Restu Kartiko Widi, Emma Savitri, Olivia Angelina, Sherlly Caroline O. J., Arief Budhyantoro

Chemical Engineering Department, University of Surabaya, Raya Kalirungkut Tenggilis, Surabaya, 60290, Indonesia
E-mail: savitri_ma@staff.ubaya.ac.id

Abstract*— TiO_2-Fe_3O_4–Bentonite photocatalytic material has been developed to inactivate of Escherichia coli. The syntheses of the TiO_2-Fe_3O_4 based photocatalyst have been carried out by sol-gel method. The bentonite used for porous support was obtained from Pacitan, Indonesia. The photocatalyst material will capture energy of UV radiation followed by the electron excitation and oxidation-reduction reactions. Because of the processes, the various types of pollutants and microorganisms can be decomposed and reduced. The electron excitation will induce the formation of hydroxyl radical and O_2. These radicals are responsible to decompose the cell wall of bacteria and further damage the bacteria's cytoplasmic membrane. Decomposing of cytoplasmic membrane causes lipid peroxidation in the membrane, and then losing their viability. It is followed by the death of bacterial cell. This study conducted a series of Escherichia coli inactivation by using photocatalyst material of TiO2-Fe_3O_4-Bentonite which was irradiated with UV light. The photocatalytic inactivation of Escherichia coli was conducted in a reactor under ultraviolet (325 nm) exposing. The photocatalytic degradation was observed for 5 hours to determine the optimum initial bacteria concentration, intensity of UV light and also photocatalyst concentration. The inactivation kinetic was approached by Chick-Watson and Hom kinetic models. The colonies calculations were conducted by Total Plate Count. The optimum condition was achieved for 300 minutes process to reach 7 bacterial log reduction units for an average bacterial inoculum size of 3.8×10^4 CFU/ml. All disinfection experiments showed a non-linear bacterial inactivation kinetic profile, which is started with shoulder lag followed by a log reduction and the tailing curve. The inactivation kinetics of Escherichia coli using TiO_2-Fe_3O_4-Bentonite photocatalytic material system satisfactorily obeyed the Hom kinetic model.

Keywords*— TiO_2; photocatalytic; disinfection; inactivation kinetics; *E.coli

I. INTRODUCTION

One of the major problems in all countries is water quality problems. The research study on water quality in the East Java found that the rivers in Surabaya contain up to 64,000 cells of Escherichia coli per 100 ml of water. The pathogenic microorganisms like Escherichia coli have caused 3.4 million people to die each year of waterborne diseases-illness [1].

The elimination of microorganisms in the wastewater through a chemical method such as the addition of chlorine is less effective and may cause harm to human health. As a result, in recent years some continuous efforts have been made to develop innovative technologies in order to remediate polluted water. Among them, photocatalysis provides a potential method because of its high efficiency, relatively low cost, non-toxic, chemically and biologically inert and also photostable [2].

TiO_2-based photocatalysts have much attention for environmental applications such as the degradation of organic pollutants, water purification, CO_2 reduction and antibacterial applications [3]–[9]. As surface coatings, TiO_2 is widely utilized as disinfecting and cleaning material. The materials have been utilized in minimizing and removing bacteria and harmful organic materials from water and air, as well as in sterilizing surfaces for places such as in medical centers [10]. On microorganism disinfections, TiO_2-based photocatalysts were used for viruses [11], bacteria [12], fungi [13], algae [14], and protozoa [15]. However, Many variety factors give effects on TiO_2 activity, such as crystal structure, surface area, nanoparticles size distribution, porosity and a number and density of hydroxyl groups on the TiO_2 surface. The forms of TiO_2 are amorphous and crystalline forms. The crystalline form is photo-catalytically active, otherwise is inactive. The crystalline forms of TiO_2 naturally are anatase, rutile, and brookite. They are different in structure. Brookite has orthorhombic structure while anatase and rutile structures are tetragonal. Anatase and rutile are more common than brookite and are easier to obtain. Anatase and rutile have high photocatalytic activity. Otherwise, brookite has never been performed for photocatalytic activity. Anatase structure is more active as a

photocatalyst than rutile structure, probably because anatase structure has the higher potential energy of photogenerated electrons and also a higher number of – OH groups on its surface [10].

In order to enhance the photocatalytic activity of TiO_2, many different modification methods have been studied, such as coupled of TiO_2 with semiconductor having lower band gap energy [16], metal-ion implanted TiO_2 [17], reduced TiOx photocatalysts [18], non-metal doped TiO_2 [19], and sensitizing of TiO_2 with dyes [20]

This study utilized Fe_3O_4 as a dopant that has a lower band gap energy and also serves to control the anatase crystal phases of TiO_2. It is responsible for the photocatalyst activity. The material was also modified by the addition of bentonite to serve as the support material to help the bacteria adsorb on to the photocatalyst surfaces. It was assessed that the combination of TiO_2-Fe_3O_4-bentonite could generate a better capability of photo degradation of dyes [7]. During photocatalysis, the reaction initiates with UV irradiation of the semiconductor. The reaction mechanism can be followed:

Photocatalyst + hν → $h_{vb}^+ + e_{cb}$
$h_{vb}^+ + OH^- (H_2O) \rightarrow OH^-$
$e_{cb}^- + O_2 \rightarrow \bullet O_2^-$
$O_2^- + H^+ \rightarrow HO_2$
$HO_2\bullet + HO_2\bullet \rightarrow H_2O_2 + O_2$
$H_2O_2 + e_{cb}- \rightarrow OH\bullet + OH$
O_2^- + reactants → products
Substrates + •OH→ products
$e_{cb}^- + OH\bullet \rightarrow OH$

The semiconductor-metal oxide can excite an electron from the filled valence band to the empty conduction band because the band gap of it is smaller than a photonic energy of UV light. This excitation of electrons from valence band to conduction band results in the formation of an excited electron and positive hole pairs. The electron can reduce oxygen from the surrounding to form superoxide radicals (•O2−) and then, with the aid of hole, singlet oxygen (1O2) can be formed. The hole can also react with water to produce hydroxyl radicals (•OH), hydrogen peroxide (H2O2), or protonated superoxide radical (•HO2). Hydrogen peroxide can further react with •OH radicals to form •HO2 [21] The decomposition of bacteria can be caused by various actions of reactive oxygen species (ROS) such as •OH, 1O2, •O2−, •O2H, H2O2. The antimicrobial action of ROS in biological systems is achieved by lipid peroxidation of the cell membrane and subsequent inactivation of the microorganisms.

Although the photocatalytic activity of TiO_2-Fe_3O_4-Bentonite has already achieved good results on the dye waste degradation [7], its photocatalytic activity in microbial disinfection still requires improvement. This investigation aimed to analyze the photocatalytic disinfection of Escherichia coli and to evaluate the effect of photocatalyst concentration, UV illumination intensity and initial concentration of bacteria concerning disinfection activity.

II. Materials and Methods

A. Materials

Materials used for the synthesis of TiO2-Fe3O4-Bentonite photocatalyst materials were TiCl4, FeCl2.4H2O, FeCl3.6H2O, TMACl, NH4OH, NaOH and ethanol and they were purchased from Sigma-Aldrich. Natural bentonite was obtained from Pacitan, East Java, Indonesia. N2 gas was supplied by Samator, Indonesia.

B. The synthesis of photocatalyst materials

The synthesis of TiO2-Fe3O4-bentonite was conducted via the sol-gel method [7]. The ratio molar of Ti: Fe was 1 : 3. The TiO2 was synthesized by dissolving TiCl4 in ethanol-water solution (1:1). The NH4OH solution was added to the mixture until pH 7. The mixture was stirred continuously for 24 hours to form a sol-gel phase. The Fe3O4 was synthesized by mixing FeCl2.4H2O, FeCl3.6H2O and NH4OH solutions in the presence of agitation and N2 gas. The Fe3O4 solid then was mixed with TMACl 2% and NaOH solution until pH 12.1. The mixture was agitated for 24 hours. After that, 140 mesh bentonite was dispersed in water for 24 hours. Then, TiO2, Fe3O4 and bentonite slurry were mixed and stirred at 50 °C for 24 hours. After stirring, the mixture was washed with water to pH 7, dried and then calcined at a temperature of 500 ºC for 6 hours.

The characterization of photocatalyst material was using XRD and SEM analysis to observe the photocatalyst phase and the morphology of the photocatalyst material. X-ray diffraction (XRD) measurements were conducted on a PANalytical PW 3373/00 X'Pert X-ray diffractometer, Netherlands, and used a CuKα, 1.54 Å, radiation at 40 kV and 30 mA. The relative intensities were recorded over the scattering range (2Θ) of 0 – 50o. The morphology and topography of photocatalyst material were observed using an SEM FEI INSPECT S-50, Netherlands. The powder was dispersed onto double-sided carbon tape and then placed in a sample holder.

C. The photodegradation of Escherichia coli

The photodegradation of Escherichia coli was carried out in a glass reactor. The observed parameters were initial bacterial concentration (103-107 CFU/mL), UV light intensity (8 – 20 lux) and also photocatalyst concentration (4 – 10 g/mL). The channels were used as a sterile airline and sample output line. The starter was introduced into the reactor containing sterile distilled water. Photocatalyst was added to a reactor at a specified concentration. The reactor was shown in figure 1. The agitation was applied to the mixture by magnetic stirrer without heating. The mixture was exposed to the UV light at λ = 325 nm at a particular intensity for 300 minutes. The sampling process was conducted every 60 minutes. The concentration of Escherichia coli in each sample were calculated through Total Plate Count (TPC) with duplication.

D. Kinetic models of bacterial inactivation

In TiO_2 catalyst applications for microbial inactivation, The most model of photo-disinfection kinetics follows the Chick-Watson (CW) model. The following is the kinetic equation of the Chick-Watson model which gives the

relationship between the number of remaining bacteria (N) and the time (t) of disinfection treatment performed:

$$\frac{N}{N_o} = exp(-kt) \quad (1)$$

where k is the disinfection rate constant and N_0 is the initial bacterial count at t = 0. In this Chick-Watson model, the reduction in the bacterial number is proportional to the time of contact with the catalyst. This correlation cannot be directly applied, as many factors influence the rate of bacterial reduction (inactivation) in the system, such as reactor configuration, inactivation model and bacterial resistance to the disinfectant used, resulting in the appearance of non-linear reduction profiles

A kinetic evaluation using the Hom model series needs to be applied to represent the photo-disinfection kinetics of E.coli. Mostly, the bacterial inactivation profile begins with (i) a less sharp early-stage bacterial lag or reduction (referred to as 'shoulder'), followed by (ii) a 'log-linear' inactivation section, and is terminated by (iii) a long process of slowing (also known as 'tailing'). In the Hom model series, there are three different empirical models based on Hom's own model - namely, the Hom model, the modified Hom model, and the Hom-Power model. The difference in these three empirical models is the sum of the empirical parameters, which are directly related to the number of nonlinearities occurring in the disinfection profile. Hom proposed an empirical Hom model after obtaining a linear curve algae-bacteria plot system:

$$log\frac{N}{No} = -kC^nT^m \quad (2)$$

where log (N / No) = log of bacterial reduction unit; N is a bacterial population at a time, t; No is the initial bacterial population; k = experiment reaction rate; C = concentration of photocatalyst used; T is the time of exposure done and m, n = empirical parameters. The empirical model with these two parameters can only explain one of the characteristics of 'shoulder' or 'tailing.'

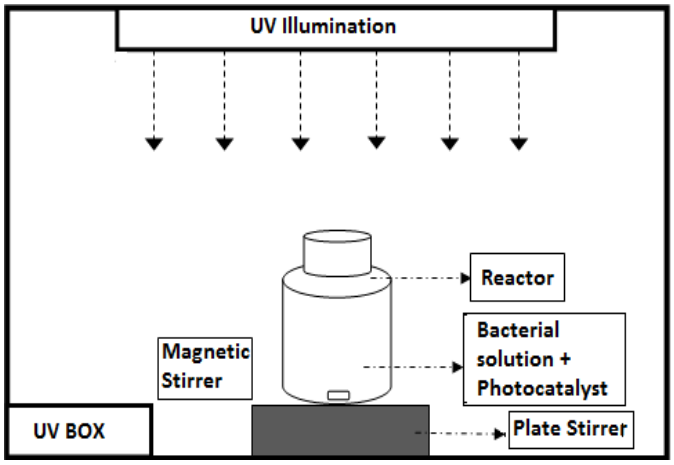

Fig. 1 The reactor used in the photodegradation of Escherichia coli

III. Results and Discussions

A. The Characterization of Photocatalyst

The catalyst used in this study was TiO_2-Fe_3O_4-Bentonite on the molar ratio of Ti: Fe = 1 : 3. By XRD characterization, the crystalline anatase phase on the photocatalyst material was obtained. The XRD and SEM analysis of the photocatalysts material can be seen in Figure 2 and 3.

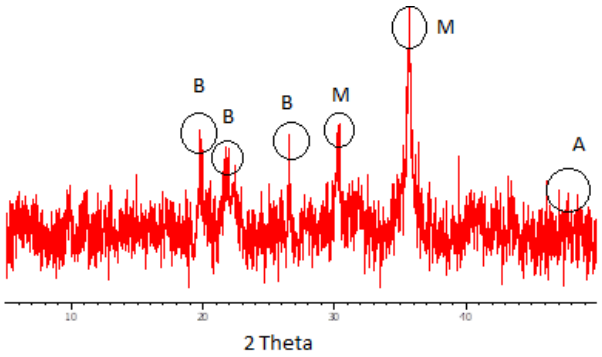

Fig. 2 X-Ray Diffraction spectrum of TiO_2-Fe_3O_4-Bentonite (with: B = Bentonite, A = TiO_2 Anatase, M = Fe_3O_4 Magnetite)

Figure 2 exhibits the strong diffraction peaks at 2θ = 30.3° and 35.8º and it refers to the crystal planes of (220) and (311) in pure Fe_3O_4 [22]. On this figure, the strong peak was seen at 2θ = 35.8° as the magnetite phase. Otherwise, Figure 2 also shows diffraction peaks at 25.2° and 47.8° exhibiting TiO_2 in the anatase phase, even the peak at 25.2 was overlapping with the bentonite peak diffraction. The intensity of magnetite is larger than anatase because Fe is more dominant than the Ti. In the XRD spectrum, it is also found the peak at 2θ = 25.8º which indicates the formation of anatase crystal plane of TiO_2 (101) [23]. The diffraction peak of TiO_2 anatase indicates that TiO_2 had been crystallized. Figure 2 also shows that the diffraction peak of photocatalyst material is broad, it indicates that the material is categorized as nanopowder. Thamapat has analyzed to compare micro powder and nanopowder of TiO_2. It showed that the nanopowder of TiO_2 is broader than that of micro powder of TiO_2 [23]. In addition, the appearance of some peaks at 2θ = 19.6º, 21.5° and 26.7º are also found in the spectrum; they indicate the diffraction characteristics of bentonite.

TABLE I
DIFFRACTION SPECTRUM OF TIO2, FE3O4, BENTONITE AND PHOTOCATALYST MATERIAL [24-26]

2Θ	TiO_2 Anatase	Magnetite	Bentonite
6.48 (Bentonite)			
19.64 (Bentonite)			19.6
21.54 (Bentonite)			21.5
25.23 (TiO_2 Anatase)	25.8		
26.66 (Bentonite)			26.7
30.21 (Magnetite)		30.3	
35.58 (Magnetite)		35.8	
43.25 (Magnetite)		43.5	
47.89 (TiO_2 Anatase)	47.8		

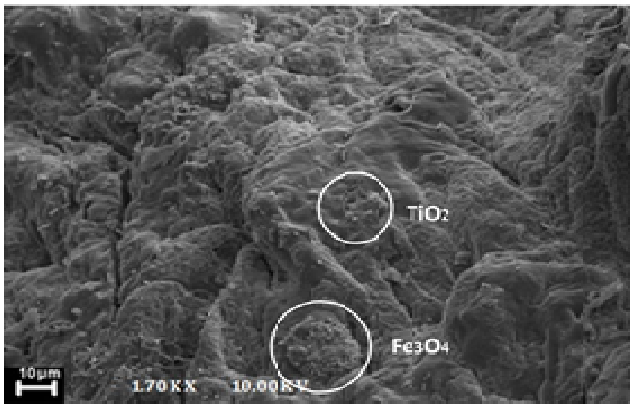

Fig. 3 The SEM of TiO_2-Fe_3O_4-Bentonite with the 1.700x magnification

The SEM analysis was performed to determine the morphological structure of the photocatalyst material. Figure 3 shows some small particles (TiO2 and Fe3O4) attached on the surface of bentonite. Figure 3 also shows that the TiO2 and Fe3O4 have not spread homogeneously on the bentonite surface. The particles are still localized in some part of bentonite. Even though the TiO2 and Fe3O4 have not attached homogenously, but the photocatalyst material of TiO2-Fe3O4-bentonite has been formed.

B. The Escherichia coli Growth

The experiments related to the disinfection rate of bacteria is valid if it is conducted at the end of the log phase of the bacterial growth curve. The condition might observe that decreasing number of Escherichia coli occurred because of the presence of the photocatalyst TiO_2-Fe_3O_4-Bentonite. Moreover, in the log phase, the disinfection rate is not disturbed by bacteria exponential growth. Escherichia coli growth curve can be seen in Figure 4. According to Fig.4, the bacteria incubation for experiments was set for 14 hours.

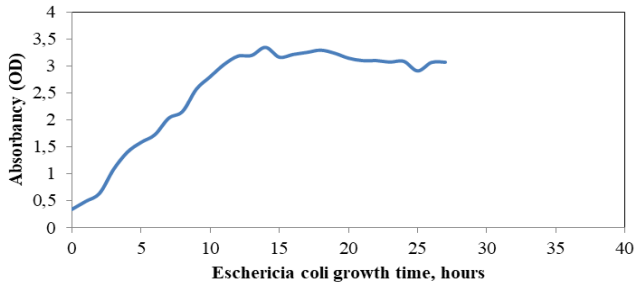

Fig. 4 Escherichia coli Growth Curve

C. The Effect of Initial Bacterial Concentration on the Photodegradation Process

On this observation, the initial concentration of bacteria of 103 up to 107 CFU/ml was designed to represent the number of bacteria commonly found in the water of the river. Figure 5 shows the effect of the initial concentration of E. coli in the water on the photo disinfection rate of E.coli using TiO2-Fe3O4-bentonite. In this study, the UV light intensity used was 20 lux, and photocatalyst concentration is as high as 10 g/L.

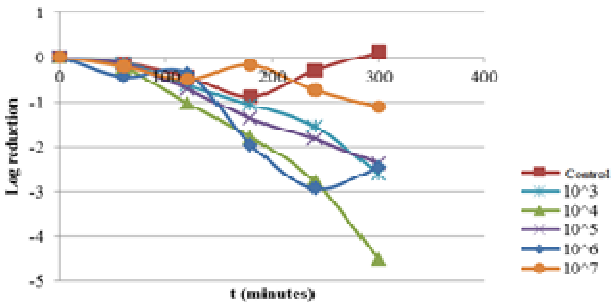

Fig.5 The effect of initial bacterial concentration on the inactivation rate of E. coli on the photocatalyst concentration of 10 gr/L and UV light intensity of 20 Lux

The control experiment used in this research was the system which has specified number of E.coli and exposed to UV light in the absence of photocatalyst. Figure 5 shows that the number of bacteria on the control system was constant during the observed time and did not decrease significantly. Figure 5 also shows that the control curve declines in the first 3 hours, and then increases in the next 2 hours. The decrease phase might be occurred due to the osmotic shock of bacteria due to the changes in the environment. The increase of bacteria in the next 2 hours indicates that the bacterias have been able to adapt to the new environment in the presence of limited nutrients. Therefore, it is found on the control curve in Figure 5 that the concentration of bacteria still increases. Thus, it can be concluded that UV light with a wavelength of 325 nm does not cause the damage or the death of the bacterial cell. From Figure 5 it can also be seen that the inactivation rate increases in the initial concentration of 103-104 CFU/ml and then decreases in line with the increasing of the initial concentration of bacteria. At the beginning of the process, the bacterial inactivation rate is slightly decreasing, but after two hours process, the significant decrease occurs. It can be explained that in the long process the active radicals produced by photocatalyst was also increasing and it is responsible for decreasing the bacteria number via destruction of bacteria cells. The photoexcitation of the semiconductor (TiO2 – Fe3O4 produced highly reactive hydroxyl radicals that ensure complete degradation of E.coli [27]. The various actions of reactive oxygen species (ROS) such as •OH, 1O2, •O2−, •O2H, H2O2 might decompose the bacteria. Lipid peroxidation of the cell membrane is occurred because of the antimicrobial action of ROS in biological systems and subsequent inactivation of the microorganisms.

The experiments for initial concentration range 103 – 107 CFU/mL can be estimated using Chick- Watson model as shown in Table 2.

Table 2 shows that the highest bacteria disinfection rate occurs at the experiment which has initial bacteria concentration of 104 CFU/mL. It indicates that the fastest rate of bacterial decline occurs at initial bacteria concentration of 104 CFU / mL. Increasing the initial bacteria concentration, it reduces the bacteria disinfection rate. On higher bacteria concentration, the photocatalyst cannot effectively damage the bacterial cells. This is due to the UV rays can not effectively to activate the photocatalyst

because of the number of bacteria on the system. The UV rays cannot easily reach the photocatalyst and produce photon to degrade the bacteria cell.

TABLE II
BACTERIA DISINFECTION RATES AND CONSTANTS FOR VARIOUS BACTERIA INITIAL CONCENTRATIONS

Initial Concentrations, CFU/mL	Chick-Watson Equation	k, $mins^{-1}$
10^3	Ln (N/N_0) = -0.0072t R^2 = 0.9069	0.0072
10^4	Ln (N/N_0) = -0,0125t R^2 = 0.9075	0.0125
10^5	Ln (N/N_0) = -0,0075t R^2 = 0,967	0.0075
10^6	Ln (N/N_0) = -0,0094t R^2 = 0,8365	0.0094
10^7	Ln (N/N_0) = -0,0031t R^2 = 0,7765	0.0031

The phenomena were proven by analyzed the turbidity of the system on the various initial bacteria concentration. The high concentration of bacteria leads to increasing fluid turbidity and causes the lack of UV rays penetrates into media. It disrupted the photocatalyst activity. The turbidity profile can be seen in Table 2. The turbidity profile was analyzed by using turbidity standard. Table 2 shows that increased bacterial concentration by ten times will make double to four-time of fluid turbidity. This fact influences on the accessibility of UV rays penetrate into the system and photoexcite the photocatalyst materials. High concentration of E. Coli will also inhibit the UV ray to reach the photocatalyst and decreases the inactivation rate of the bacteria.

TABLE III
ABSORBANCE VALUE OF STARTERS IN VARIOUS INITIAL BACTERIAL CONCENTRATION

Absorbance (OD)	Bacterial concentration (CFU/ml)
0.00254	10^3
0.00535	10^4
0.03476	10^5
0.05557	10^6
0.22325	10^7

D. The Effect of UV Light Intensity on the Photodegradation

Photocatalyst requires light energy to activate sufficiently. In this research, the UV light intensity was observed to observe the effect of UV light intensity on the photocatalytic activity. The UV light intensity affected the performance of on TiO_2 catalyst on the reaction. The effect of intensity can be observed from the inactivation constants (disinfection constants), which is the value of the curve slope. The greater curve slope meant the greater the inactivation rate and the inactivation of *E. coli* in the water because of photocatalyst was more effective.

From Figure 6, it can be seen that the number of bacteria reduction increase in line with increasing the intensity of UV light. This is due to the surface area of the photocatalyst receive more energy for higher intensity to promote the electrons excitation process.

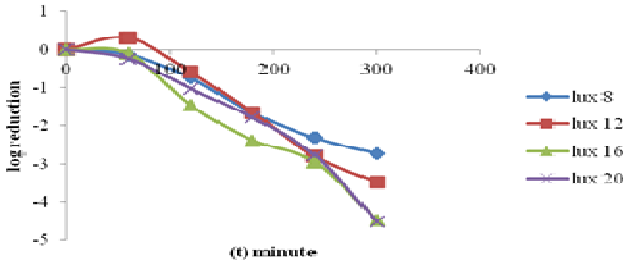

Fig. 6 The effect of UV light intensity on the rate of E. coli inactivation with the catalyst concentration of 10 gr/L and initial bacteria concentration 104CFU/ml

E. The Effect of Photocatalyst Concentration on the Photodegradation Process

The influence of the photocatalyst concentration on to bacteria reduction can be seen in Figure 7. Figure 7 shows that the optimum E.coli inactivation occurs at photocatalyst concentrations 4 g/L. Meanwhile, at a concentration 7 g/L and 10 g/L, the numbers of E. coli reduction were not different significantly. It can be caused by obstruction due to the scattering of UV light by the photocatalyst material at the higher concentration so that the photocatalyst material were not activated by UV light.

The increasing concentrations of TiO2 photocatalysts loaded in a stirred reactor can increase turbidity, thereby reducing the penetration of UV rays [28]. In the case of TiO2 catalyst, it has been observed the occurrence of the photocatalyst aggregation in the reactor. Helali et al. explained this phenomenon by DLS (Dynamic Light Scattering) analysis and showed that the photocatalyst concentration in the reactor could lead to an increase in the size of the agglomerates when its concentration was higher. It has led to the photocatalyst reduction due to the light penetration reduction. Additionally, agglomerated catalyst leads to reduced catalyst surface area so that the active sites of the catalyst are also reduced.

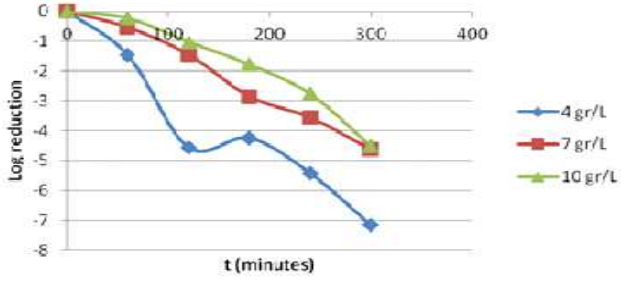

Fig. 7 The effect of photocatalyst concentration on the rate of E. coli inactivation with the UV light intensity 16 lux and initial bacteria concentration 104CFU/ml

Rincon et al. also explained that at the higher TiO2 concentration, the reaction led to reducing photocatalyst efficiency due to the final photocatalytic process. The reaction is followed :

$OH^* + OH^* \rightarrow H_2O_2$

$H_2O_2 + OH^* \rightarrow H_2O + HO_2^*$

In reaction (1), a lot of radical OH* can dimerize to form H2O2; then it was formed HO2* in the reaction (2) which is less reactive than the OH *.

F. The Photodegradation Kinetic Models

Photodisinfection curve of E.coli by photocatalyst TiO2-Fe3O4-Bentonite generally consists of a log-linear phase. In this study, the kinetic models evaluated by Chick-Watson and Hom kinetics models. Both kinetic models were analyzed on their optimum conditions. Both models were applied on the assumption that the concentration of disinfectant was constant during the whole disinfection process. Figure 8 shows a comparison between both kinetics models

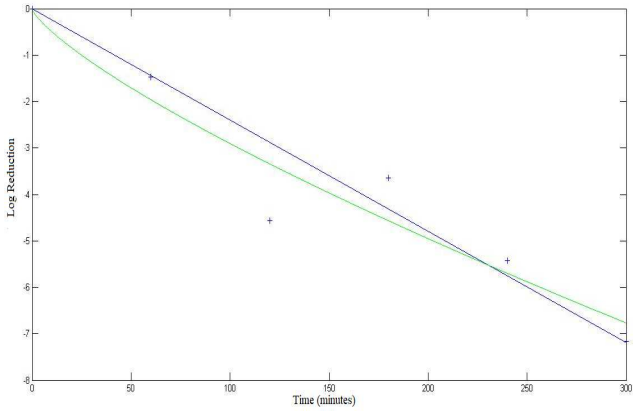

Fig. 8 The kinetics model of Chick-Watson and Hom, (the green line = Hom model; blue line = Chick-Watson model; and a + = raw data on the optimum conditions)

Figure 8 shows that the Hom model gives the best suitability of the disinfection kinetic of E.coli. It is caused that Hom models considered the variables that affecting the disinfection process, such as time and the catalyst used.

TABLE IV
THE PARAMETER KINETICS OF CHICK-WATSON AND HOM MODELS

Kinetic Model	k	m	n	R^2
Chick-Watson	0,0239	-	-	0,9007
Hom	0,338	0,7703	-1,008	0,9182

The parameter kinetics of bacterial disinfection can be seen in Table 4. The higher constant value of bacterial disinfection (k) indicates that the rate of bacterial disinfection occurred faster. The m and n constants in Hom model respectively show the influence of time and concentration of photocatalyst in the reduction process of bacteria. When m values < 1, it indicates that a 'tailing' was occurring in the curve, which means that the disinfection rate began to decline over time due to the competition of the photocatalysis of bacteria that are still active with the organic compounds formed by the lysis of bacterial cells that have been damaged [29]. In addition, when the value of n < 1, it indicates that the concentration of the photocatalyst in the system does not significantly affect the disinfection process because the concentration of TiO2 did not change over time. The values of R2 demonstrates the suitability of data compared to models. The R2 for Hom model is 0.9182, and it is higher than that of the Chick-Watson model. This shows that the kinetics of disinfection of E.coli by the photocatalyst material of TiO2-Fe3O4-Bentonite is more appropriate with the Hom model.

IV. CONCLUSIONS

Escherichia coli photo-disinfection kinetics has been successfully achieved in this study. A total of 7 bacterial log reduction can be achieved in 300 minutes by exposing with UV light. The optimum conditions were obtained when the initial bacteria concentration of 104 CFU/mL, the photocatalyst concentration of 4 g/L and UV light intensity of 16 lux. All disinfection experiments showed a non-linear bacterial inactivation kinetic profile, which is started with shoulder lag followed by a log reduction and the tailing curve. Hom models more represent the disinfection kinetics model in this study.

ACKNOWLEDGMENT

The authors are thankful for the financial support of Directorate of Research and Community Service, Directorate General Strengthening Research and Development, Indonesian Ministry of Research, Technology and Higher Education no: 120/SP2H/LT/DRPM/IV/2017 on 3 April 2017 through HIKOM Grant 2017.

REFERENCES

[1] The United Nations World Water Development Report, Water, and energy, 2014.

[2] K. Ubonchonlakate, L. Sikonga, F. Saito, "Photocatalytic disinfection of P. aeruginosa bacterial Ag-doped TiO_2 film,". *Procedia Engineering*, vol. 32, pp. 656–662, 2012

[3] X.Z. Li, H. Liu, L.F. Cheng, H.J. Tong, " Photocatalytic oxidation using a new catalyst TiO_2 microsphere for water and wastewater treatment," *Environ. Sci. Technol.* Vol. 37, pp. 3989-3994, 2003

[4] H. Oveisi, S. Rahighi, X. Jiang, Y. Nemoto, A. Beitollahi, S. Wakatsuki, Y. Yamauchi, "Unusual antibacterial property of mesoporous titania films: drastic improvement by controlling surface area and crystallinity," *Chem. Asian J.*, vol. 5, pp. 1978-1983, 2010

[5] M. Pelaez, N.T., Nolan, S.C., Pillai, M.K. Seery, P. Falaras, A.G. Kontos, P.S.M. Dunlop, J.W.J., Hamilton, J.A. Byrne, K. O'Shea, M.H., Entezari,D.D. Dionysiou, "A review on the visible light active titanium dioxide photocatalysts for environmental Applications." *Appl. Catal. B: Environ.* Vol. 125, pp. 331-349, 2012

[6] J. Zhao, X. Yang, "Photocatalytic oxidation for indoor air purification: a literature review," *Build. Environ.* vol. 38, pp. 645-654, 2003

[7] R.K. Widi, A. Budhyantoro, E. Savitri, "Use of TiO_2-Fe_3O_4 pillared bentonite as photocatalyst in photodegradation of basic blue," *Journal of Chemical and Pharmaceutical Research*, vol. 7, pp. 183-187, 2015

[8] R.K. Widi, A. Budhyantoro, "Catalytic performance of TiO_2-Fe_3O_4 supported bentonite for photocatalytic degradation of phenol," *International Journal of Applied Engineering Research*, 2014

[9] E. Savitri, R.K. Widi, A. Budhyantoro, "The effect of the calcinations temperature during synthesis of TiO_2-Fe_3O_4-bentonite as photocatalyst material," *Journal of Chemical and Pharmaceutical Research*, 2015

[10] M. Hasmaliza, H. S. Fooa and K. Mohd, "Anatase as Antibacterial Material in Ceramic Tiles," *Procedia Chemistry*, vol. 19, pp. 828 – 834, 2016

[11] M. Cho, H. Chung, W. Choi, J. Yoon, "Different inactivation behaviors of MS-2 phage and Escherichia coli in TiO2 photocatalytic disinfection," *Appl. Environ. Microbiol.* Vol. 71, pp. 270-275, 2005

[12] A.G. Rincón, C. Pulgarin, C. “Effect of pH, inorganic ions, organic matter and H_2O_2 on E. coli K12 photocatalytic inactivation by TiO_2: implications in solar water disinfection,” *Appl. Catal. B: Environ.* Vol. 51, pp. 283-302. 2004

[13] C. Maneerat, Y. Hayata, “Antifungal activity of TiO_2 photocatalysis against Penicillium expansum in vitro and in fruit tests,” *Int. J. Food Microbiol.* Vol. 107, pp. 99-103. 2006

[14] J.R. Peller, R.L. Whitman, S. Griffith, P. Harris, C. Peller, J. Scalzitti, “TiO_2 as a photocatalyst for control of the aquatic invasive alga, Cladophora, under natural and artificial light,” *J. Photochem. Photobiol. A: Chem.* Vol. 186, pp. 212-217. 2007

[15] V. Aruoja, S. Pokhrel, M. Sihtmae, M. Mortimer, L. Madler, A. Kahru, “Toxicity of metal-based nanoparticles to algae, bacteria and protozoa, *Environ. Sci. Nano*,” vol. 2, pp. 630-644, 2005

[16] T. Hirai, K. Suzuki, I. Komasawa, “Preparation and photocatalytic properties of composite CdS nanoparticles–titanium dioxide particles,” *J. Colloid Interface Sci.* Vol. 244, pp. 262-265. 2001

[17] A.L. Stepanov, “Applications of ion implantation for modification of TiO_2: a review,” *Rev.Adv.Mater. Sci.* Vol. 30, pp. 150-165. 2012

[18] T. Ihara, M. Miyoshi, M. Ando, S. Sugihara, Y. Iriyama, “Preparation of a visible light-active TiO_2 photocatalyst by RF plasma treatment, “ *J. Mater. Sci.* Vol. 36, pp. 4201-4207, 2001

[19] C. Di Valentin, G. Pacchioni, “ Trends in non-metal doping of anatase TiO_2: B, C, N, and F,” *Catal. Today*. Vol. 206, pp. 12-18., 2013

[20] C.Y., Lee, J.T. Hupp, J.T. “Dye-sensitized solar cells: TiO_2 sensitization with a bodipyporphyrin antenna system,” *Langmuir*. Vol. 26 (5), pp. 3760–3765, 2010

[21] J. Schneider, M. Matsuoka, M. Takeuchi, J. Zhang, Y. Horiuchi, M. Anpo, D.W. Bahnemann, Chem. Rev. Vol. 114, pp. 9919-9986, 2014

[22] P.L. Hariani, “Synthesis and Properties of Fe_3O_4 Nanoparticles by Co-precipitation Method to Removal Procion Dye,” *International Journal of Environmental Science and Development*, vol. 4, pp. 33-37, 2013

[23] K. Thamaphat, et al., “Characterization of TiO_2 Powder by XRD and TEM”, *Kasetsart J.*, vol. 42, pp 358-359, 2008

[24] Boutra, B. dan Trari, M. 2016. Solar photodegradation of a textile azo dye using synthesized ZnO/Bentonite. *Water Science and Technology*, 5, 1211-1220.

[25] Cai, Y., Stromme, M., dan Welch, K. 2013. Photocatalytic antibacterial effects are maintained on resin-based TiO2 nanocomposite after cessation of UV irradiation. PLoS ONE.

[26] Chen, D., Tang, Q., Li, X., Zhou, X., Zang, J., Xue, W. Q., Xiang, J.Y., dan Guo, C. Q. 2012. Biocompatibility of magnetic Fe3O4 nanoparticles and their cytotoxic effect on MCF-7 cells. *International Journal Nanomedicine*.

[27] Rahma Hendili , Abir Alatrache, Mossadok Ben-Attia, Marie-No€elle Pons Antibacterial inactivation of spiramycin after titanium dioxide photocatalytic treatment, C. R. Chimie 20 (2017) 710 – 716

[28] S. Helali *et al.*, “Solar photocatalysis: A green technology for E. coli contaminated water disinfection. Effect of concentration and different types of suspended catalyst,” *J. Photochem. Photobiol. A Chem.*, vol. 276, pp. 31–40, 2014.

[29] M. N. Chong, B. Jin, C. W. K. Chow, and C. Saint, “Recent developments in photocatalytic water treatment technology: a review,” *Water Res.*, vol. 44, no. 10, pp. 2997–3027, 2010.